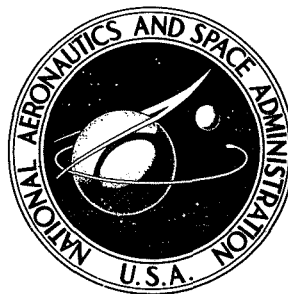


078103

74-17343

TDL 75-10099

NASA TECHNICAL NOTE



NASA TN D-7842

NASA TN D-7842

HQ SAMTEC, AFL 2827
TECHNICAL LIBRARY (PMET)
VANDENBERG AFB, CA 93437

MINIMIZATION OF SONIC-BOOM PARAMETERS IN REAL AND ISOTHERMAL ATMOSPHERES

Christine M. Darden

Langley Research Center

Hampton, Va. 23665



NATIONAL AERONAUTICS AND SPACE ADMINISTRATION • WASHINGTON, D. C. • MARCH 1975

1. Report No. NASA TN D-7842	2. Government Accession No.	3. Recipient's Catalog No.	
4. Title and Subtitle MINIMIZATION OF SONIC-BOOM PARAMETERS IN REAL AND ISOTHERMAL ATMOSPHERES		5. Report Date March 1975	
		6. Performing Organization Code	
7. Author(s) Christine M. Darden		8. Performing Organization Report No. L-9810	
9. Performing Organization Name and Address NASA Langley Research Center Hampton, Va. 23665		10. Work Unit No. 743-35-31-02	
		11. Contract or Grant No.	
12. Sponsoring Agency Name and Address National Aeronautics and Space Administration Washington, D.C. 20546		13. Type of Report and Period Covered Technical Note	
		14. Sponsoring Agency Code	
15. Supplementary Notes			
16. Abstract <p>The procedure for sonic-boom minimization introduced by Seebass and George for an isothermal atmosphere has been converted for use in the real atmosphere by means of the appropriate equations for sonic-boom pressure signature advance, ray-tube area, and acoustic impedance. Results of calculations using both atmospheres indicate that except for low Mach numbers or high altitudes, the isothermal atmosphere with a scale height of 7620 m (25 000 ft) gives a reasonable estimate of the values of overpressure, impulse, and characteristic overpressure obtained by using the real atmosphere. The results also show that for aircraft design studies, propagation of a known F-function, or minimization studies at low supersonic Mach numbers, the isothermal approximation is not adequate.</p> <p style="text-align: right;">PRICES SUBJECT TO CHANGE</p>			
17. Key Words (Suggested by Author(s)) Sonic-boom minimization Impulse Characteristic overpressure Equivalent area Pressure signature		18. Distribution Statement Unclassified - Unlimited New Subject Category 05	
19. Security Classif. (of this report) Unclassified	20. Security Classif. (of this page) Unclassified	21. No. of Pages 31	22. Price* \$ 3.75

* For sale by the National Technical Information Service, Springfield, Virginia 22151

MINIMIZATION OF SONIC-BOOM PARAMETERS IN REAL AND ISOTHERMAL ATMOSPHERES

Christine M. Darden
Langley Research Center

SUMMARY

The procedure for sonic-boom minimization introduced by Seebass and George for an isothermal atmosphere has been converted for use in the real atmosphere by means of the appropriate equations for sonic-boom pressure signature advance, ray-tube area, and acoustic impedance. Results of calculations using both atmospheres indicate that except for low Mach numbers or high altitudes, the isothermal atmosphere with a scale height of 7620 m (25 000 ft) gives a reasonable estimate of the values of overpressure, impulse, and characteristic overpressure obtained by using the real atmosphere. The results also show that for aircraft design studies, propagation of a known F-function, or minimization studies at low supersonic Mach numbers, the isothermal approximation is not adequate.

INTRODUCTION

The sonic boom is recognized as being one of the major problems confronting the advancement of high-speed aircraft. One approach to the reduction of this annoyance is through boom-configured aircraft in which low sonic-boom requirements become a fundamental constraint at the outset of aircraft design. This design constraint is embodied in the equivalent area distribution which relates the aircraft to its sonic-boom pressure signature and therefore specifies the lengthwise development of aircraft lift and volume required to produce desired sonic-boom characteristics. Appropriate equivalent area distributions can be obtained from the method of Seebass and George (ref. 1), which minimizes various parameters of the pressure signature from a cruising aircraft in an isothermal atmosphere for a given weight, altitude, and Mach number and defines the F-function and equivalent area distribution required to produce this signature. To provide the same capability in the real atmosphere, the method of reference 1 has been modified herein by the appropriate equations (ref. 2) for signature advance, ray-tube area, and acoustic impedance. The present study includes pressure signatures in which the impulse, initial shock, and maximum overpressure have been minimized. Comparisons of predictions for these parameters and of pressure signatures, F-functions, and equivalent area distributions from both atmospheres are shown.

SYMBOLS

Although values are given in both SI and U.S. Customary Units in this report, the measurements and calculations for the investigation were made in U.S. Customary Units.

A	ray-tube area
A_e	equivalent area
A_ℓ	equivalent area at equivalent length ℓ
a	speed of sound
B	slope of rise in F-function
C	height of F-function at balance point
D	constant in F-function equation
F	Whitham F-function
G	area of function to front balance point
H	scale height
h	airplane altitude
I	impulse of pressure signature, $\int_{P>0} P dt$
K	reflection factor
ℓ	equivalent length of airplane
M	Mach number
P	pressure perturbation

Δp	overpressure
Δp_c	characteristic overpressure, $4I/t_t$
p_a	ambient pressure
s	slope of balancing line
t	time
t_t	total time between bow and rear shocks in pressure signature
V	speed
W	airplane weight
x, y	axial distances
y_f	axial position of front area balancing
y_r	position of rear area balancing in F-function
z	vertical distance from airplane axis
α	advance of acoustic rays
$\beta = (M^2 - 1)^{1/2}$	
γ	ratio of specific heats, 1.4 for air
$\Gamma = \frac{\gamma + 1}{2}$	
δ	Dirac delta function
λ	axial position at which F-function becomes negative
ρ	density

Subscripts:

f	front shock
g	ground
h	altitude of initial waveform
J	minimum impulse signature
max	maximum pressure in minimum shock signature
r	rear shock
s	minimum shock signature
so	minimum overpressure signature

A double prime indicates a second derivative with respect to distance.

METHOD

At distances from an aircraft where all the characteristics of a pressure signature have coalesced into bow and rear shocks of equal strengths, Jones showed that the lower bound shock strength required the F-function to have the form of a Dirac delta function at $x = 0$ (ref. 3). He later (ref. 4) extended this conclusion to the bow shocks of N-wave signatures in which the bow and rear shocks were of unequal strengths. However, shape changes required in current supersonic transports to approach these lower bounds resulted in prohibitively high drag penalties (ref. 5). McLean (ref. 6) observed that with a sufficiently long airplane, the signature reaching the ground will not have attained its N-wave form. Hayes (ref. 7) also pointed out that in the real atmosphere, characteristics coalesce more slowly than in the uniform atmosphere and the shape of the signature "freezes"; this increases the possibility of the midfield signature shape reaching the ground. This phenomenon led George (ref. 8) to consider signatures which differ from the basic N-wave form. He showed that the lower bounds for the bow shock of these signatures also required the F-function to be characterized by a delta function at $x = 0$.

The minimizing form of the F-function in these cases and the observation that the effective length available for bow shock minimization is reduced when the rear shock is

also constrained led to the F-function assumed by Seebass and George in their minimization of the entire signature (fig. 1). Most of the equations which follow were developed by Seebass and George (ref. 1) and are repeated here for convenience.

The assumed form of the minimizing F-function is

$$\left. \begin{aligned} F(y) &= G\delta(y) + By + C & (0 \leq y \leq \lambda) \\ F(y) &= By - D & (\lambda \leq y \leq \ell) \end{aligned} \right\} \quad (1)$$

In these equations G , B , C , D , and λ are unknown coefficients which are determined by the cruise conditions of the aircraft, by the prescribed ratio of bow to rear shock, and by the parameter of the signature which is being minimized. The Whitham function $F(y)$ represents the shape characteristics of the pressure signature and is defined in reference 9 in terms of the equivalent area distribution as

$$F(y) = \frac{1}{2\pi} \int_0^y \frac{A_e''}{(y-x)^{1/2}} dx \quad (2)$$

Equation (2) is an Abel integral equation which may be inverted to give the function $A_e(x)$ in terms of the F-function. When this function is evaluated at ℓ , the result is

$$A_e(\ell) = 4 \int_0^\ell F(y) (\ell - y)^{1/2} dy \quad (3)$$

Upon substituting the minimizing form of the F-function into equation (3) and integrating, the following equation for the development of cross-sectional area is obtained:

$$A_e(x) = 4Gx^{1/2} + \frac{16}{15} Bx^{5/2} + \frac{8}{3} Cx^{3/2} - 1(x - \lambda) \frac{8}{3} (C + D)(x - \lambda)^{3/2} \quad (4)$$

where $1(x - \lambda)$ is the Heaviside unit step function.

If the effects of aircraft wake and engine exhaust are neglected and if the aircraft volume is zero at its base, then the area at ℓ is entirely due to cruise lift or

$$\frac{\beta W}{\rho V^2} = 4G\ell^{1/2} + \frac{16}{15} B\ell^{5/2} + \frac{8}{3} C\ell^{3/2} - \frac{8}{3} (C + D)(\ell - \lambda)^{3/2} \quad (5)$$

In an isothermal atmosphere $\frac{p_{a,h}}{p_{a,g}} = e^{-h/H}$, where H is the pressure scale height. If this approximation is used in equation (5), then

$$\frac{\beta W}{\rho V^2} = \frac{\beta W}{\gamma M^2 p_a} = \frac{\beta W}{\gamma M^2 p_{a,g} e^{-h/H}}$$

for the isothermal atmosphere.

Because the linear pressure signal propagates down the ray tube at the local speed of sound and each point of the signal advances according to its amplitude, the signal is distorted at the ground and would be generally multivalued. Shocks are located in this distribution by the area-balancing technique (ref. 10). For the purpose of illustrating area balancing, the value of B is zero in figure 2. The first constraint imposed upon $F(y)$ is that front area balancing must occur at $y = y_f$, where y_f is the first point at which $F(y) = C$; that is

$$\int_0^{y_f} F(y) dy = G = \frac{\alpha y_f}{2} F(y_f) = \frac{\alpha y_f}{2} C \quad (6)$$

For the real atmosphere, the advance (ref. 2) of any point of the signal is given by

$$\alpha_y = \frac{\Gamma M_h^3 F(y)}{(2\beta)^{1/2}} \int_0^z \frac{p_{a,h}}{p_a} \left(\frac{\rho_{a,h}}{\rho_h a} \right)^{1/2} \left(\frac{A_h}{z_h A} \right)^{1/2} \frac{M}{\beta} dz \quad (7)$$

where z is the vertical distance of the signal from the airplane axis, z_h is the vertical distance of the initial waveform from the aircraft axis, A and A_h are ray-tube areas determined from

$$\frac{A_h}{z_h A} = \frac{1}{M_h \left[1 - \frac{1}{M(z)^2} \right]^{1/2} \int_0^z \frac{dz}{[M(z)^2 - 1]^{1/2}} \quad (8)$$

and $\Gamma = \frac{\gamma + 1}{2}$. The initial waveform must be defined away from the airplane because the F -function can only represent the body shape accurately at several body lengths away and the acoustical theory used in describing the propagation of the signal fails near the aircraft. The slope of the balancing line is proportional to the reciprocal of the advance at any point of the signal; thus

$$s = \frac{(2\beta)^{1/2}}{\Gamma M_h^3 \int_0^z \frac{p_{a,h}}{p_a} \left(\frac{\rho_{a,h}}{\rho_h a}\right)^{1/2} \left(\frac{A_h}{z_h A}\right)^{1/2} \frac{M}{\beta} dz} = \frac{F(y)}{\alpha_y} \quad (9)$$

For the rear area balancing to occur between points ℓ and y_r then,

$$\int_{\ell}^{y_r} F(y) dy = \frac{1}{2} [B\ell - D + F(y_r)] (y_r - \ell) \quad (10)$$

where y_r is the unknown second intersection point of the rear area-balancing line with $F(y)$. (See fig. 1.) If a cylindrical wake is assumed, $F(y)$ and its integral for $y > \ell$ can be expressed in terms of $F(y)$ for $y < \ell$ according to reference 11 as follows:

$$F(y) = - \frac{1}{\pi(y - \ell)^{1/2}} \int_0^{\ell} \frac{(\ell - x)^{1/2}}{y - x} F(x) dx \quad (y > \ell) \quad (11)$$

$$\int_{\ell}^{y_r} F(y) dy = - \frac{2}{\pi} \int_0^{\ell} F(x) \tan^{-1} \left(\frac{y_r - \ell}{\ell - x} \right)^{1/2} dx \quad (y > \ell) \quad (12)$$

It is necessary to define $F(y)$ and its integral for $y > \ell$ in this way for optimization problems since aircraft geometry, and thus the Whitham function, can be varied arbitrarily only in the range $0 \leq y \leq \ell$.

The constraint on the ratio of shocks is given by

$$\frac{P_f}{P_r} = \frac{C}{D - B\ell + F(y_r)} \quad (13)$$

To insure that y_r is an intersection point of $F(y)$ and the balancing line, then

$$F(y_r) = s(y_r - \ell) + B\ell - D \quad (14)$$

and the slope of $F(y)$ at y_r must be less than s .

Solving the system of equations (5), (6), (10), (13), and (14) provides values for the constants G , C , D , λ , and y_r . Types of signatures studied include flat-topped signatures in which overpressure is minimized and $B = 0$ and signatures in which $F(y)$ is allowed to rise between y_f and λ , with a resulting minimum shock followed by a pressure rise (fig. 3). The value of B in this form of $F(y)$ may range between 0 and s .

With the values of the coefficients known, the minimizing F-function and area distributions may be determined by equations (1) and (4).

To convert $F(y)$ into pressure near the airplane, the following equation is used:

$$\left(\frac{P}{p_a}\right)_h = \frac{\gamma M^2 F}{(2\beta z_h)^{1/2}} \quad (15)$$

The isothermal approximation was used by Seebass and George in the propagation of this pressure distribution to the ground. By using linear theory for the real atmosphere, the Rayleigh acoustic energy is conserved along acoustic rays and, thus,

$$P_g = \left(\frac{A_h}{A_g}\right)^{1/2} \left(\frac{\rho_g a_g}{\rho_h a_h}\right)^{1/2} P_h \quad (16)$$

Finally, by using a ground reflection factor K , the pressure perturbations are converted into the ground signature by

$$\Delta p_g = P_g K \quad (17)$$

DISCUSSION

Except where indicated otherwise, all results shown are for the following conditions: Mach number, 2.7; altitude, 18 288 m (60 000 ft); weight, 272 155 kg (600 000 lb); equivalent length, 91.44 m (300 ft); reflection factor, 2.0; scale height, 7620 m (25 000 ft); ratio of bow-to-rear shock pressure, 1.

The minimizing F-functions, pressure signatures, and equivalent areas obtained by using the same input conditions for the isothermal atmosphere and the real atmosphere are shown in figures 4, 5, and 6, respectively. Notice that even though the level of the F-function predicted by the isothermal atmosphere is low (fig. 4), the isothermal pressure signature (fig. 5) gives an excellent prediction of the shock level. Thus, the error introduced in using the isothermal atmosphere to calculate the F-function must, in part, be canceled out by using the isothermal atmosphere for signature propagation also. The lengths of the signatures (fig. 5) do differ; this indicates possible error in those parameters which vary with the length or area of the pressure signature. Use of the isothermal substitution for $\beta W/\rho V^2$ results in an area distribution whose total area A_ℓ is too low to reflect cruise weight requirements at the given Mach number and altitude in the real atmosphere. For the same Mach number and altitude then, the isothermal areas shown

in figure 6 actually represent a significantly lighter weight airplane. This lower weight also explains the lower level of the F-function in figure 4.

The F-functions obtained for both the isothermal and the real atmospheres were input into the real atmosphere sonic-boom program of reference 12, and the results from this program were compared with the results predicted by the isothermal atmosphere and real atmosphere minimization programs. A much lower shock is predicted by the program of reference 12 than by the isothermal minimization program, as shown in figure 7. This result supports the statement that the F-function predicted by the isothermal atmosphere represents a smaller airplane, but this F-function, when also propagated through an isothermal atmosphere, nearly corrects itself to give good predictions of the shock levels for the input conditions. Figure 8 shows that the real atmosphere minimization program and the program of reference 12 predict identical pressure signatures on the ground.

The isothermal prediction of shock levels using a scale height of 7620 m (25 000 ft) is satisfactory but the resulting equivalent area distributions cannot be used for aircraft design studies. The problem arises because the isothermal approximation gives the incorrect pressure at flight altitudes, and this leads to an error in total lift. Within the isothermal approximation, this error could be alleviated by using the correct pressure in the total lift expression (eq. (5)) or by using the scale height which gives the correct pressure at that altitude. For the given input conditions, the area distribution can be corrected to within 4 percent of the real distribution by using equation (5) and to within 2 percent by using the scale height, but the resulting shock level predictions are about 20 percent and 8 percent too large. Thus, it appears that the isothermal atmosphere minimization program using a scale height of 7620 m (25 000 ft) is more accurate in predicting the shock level. The corresponding area distribution may be improved by the factor $A_{\ell, \text{real}}/A_{\ell, \text{isothermal}}$. In figure 9, this ratio is plotted as a function of altitude for a scale height of 7620 m (25 000 ft). After correction, the isothermal area distribution differs by less than 8 percent from the real distribution (fig. 10). It should be noted, however, that when this corrected area distribution was propagated through the real atmosphere, the resulting shock level was about 5 percent greater than that given by the real atmosphere; this emphasizes the sensitivity of shock level to the shape of the equivalent area growth.

For comparison purposes, the far-field minimum impulse results of Jones (ref. 4) have also been modified by the appropriate equations for the real atmosphere, and the results for the three types of signatures (fig. 3) are shown in figures 11 and 12. Ground overpressure as a function of Mach number, equivalent length, altitude, and airplane weight is presented in figure 11 for the real and isothermal atmospheres. Values of B in the minimum shock signature are taken to be $s/2$. Smaller values of the shock Δp_s

are obtained in this signature as $B \rightarrow s$ or as the signature approaches an N-wave. It is believed, however, that values of B too close to s give signatures which are indistinguishable from high-strength N-waves. There is generally good agreement between the real atmosphere and isothermal atmosphere results for the shock levels in both the minimum overpressure and minimum shock signatures except at the lower Mach numbers where the sonic speed gradient in the real atmosphere causes significant changes in the ray-tube area (ref. 2) which are not accounted for in the isothermal atmosphere approximation. The difference in the predictions for $\Delta p_{g,J}$ and $\Delta p_{g,max}$ can be explained by the difference in the advance of the two atmospheres.

The predicted impulses for the real and isothermal atmospheres are presented in figure 12. Because of the greater advance, and therefore greater signature length, the real atmosphere predictions are higher than the isothermal atmosphere predictions. The isothermal predictions for impulse are within 10 percent of the values predicted by the real atmosphere with the exception of those at low Mach numbers or high altitudes, where significant error occurs. Again, these differences are explained by the greater effect of the speed of sound gradient at low Mach numbers and by the error (which increases with altitude) in the isothermal advance of the signal.

In an effort to define a parameter which includes the effects of both shocks and impulse, Warren (ref. 13) introduced the characteristic overpressure, defined as $4I/t_t$ where I is the impulse of the pressure signature and t_t is the total time in seconds between the bow and rear shocks in the pressure signature. With this definition, the characteristic overpressure agrees with the traditional definition of overpressure for the far-field N-wave. Figure 13 presents the characteristic overpressures for the minimum shock and minimum overpressure signatures. Isothermal atmosphere predictions for Δp_c give a reasonable estimate of values predicted by the real atmosphere. Real atmosphere predictions for Δp_c are generally lower because of the longer signatures in the real atmosphere.

CONCLUDING REMARKS

The method of Seebass and George for sonic-boom minimization in an isothermal atmosphere has been modified for use in a real atmosphere. Comparisons of results for both atmospheres indicate that for a given length, weight, altitude, and Mach number, the isothermal approximation with a scale height of 7620 m (25 000 ft) gives a good estimate of shock strength. The equivalent area distribution resulting from the isothermal atmosphere, however, is unrealistically low but may be improved by a simple factor so that the

correct distribution is predicted to within 8 percent. Results also show that for aircraft design studies, propagation of a known F-function, or minimization studies at low supersonic Mach numbers, the isothermal approximation is not adequate.

Langley Research Center,
National Aeronautics and Space Administration,
Hampton, Va., January 24, 1975.

REFERENCES

1. Seebass, R.; and George, A. R.: Sonic-Boom Minimization. *J. Acoust. Soc. America*, vol. 51, no. 2, pt. 3, Feb. 1972, pp. 686-694.
2. George, A. R.; and Plotkin, Kenneth J.: Sonic Boom Waveforms and Amplitudes in a Real Atmosphere. *AIAA J.*, vol. 7, no. 10, Oct. 1969, pp. 1978-1981.
3. Jones, L. B.: Lower Bounds for Sonic Bangs. *J. Roy. Aeronaut. Soc.*, vol. 65, no. 606, June 1961, pp. 433-436.
4. Jones, L. B.: Lower Bounds for Sonic Bangs in the Far Field. *Aeronaut. Quart.*, vol. XVIII, pt. 1, Feb. 1967, pp. 1-21.
5. Carlson, Harry W.: Influence of Airplane Configuration on Sonic-Boom Characteristics. *J. Aircraft*, vol. 1, no. 2, Mar.-Apr. 1964, pp. 82-86.
6. McLean, F. Edward: Some Nonasymptotic Effects on the Sonic Boom of Large Airplanes. NASA TN D-2877, 1965.
7. Hayes, Wallace D.: Brief Review of the Basic Theory. *Sonic Boom Research*, A. R. Seebass, ed., NASA SP-147, 1967, pp. 3-7.
8. George, A. R.: Lower Bounds for Sonic Booms in the Midfield. *AIAA J.*, vol. 7, no. 8, Aug. 1969, pp. 1542-1545.
9. Whitham, G. B.: The Flow Pattern of a Supersonic Projectile. *Commun. Pure & Appl. Math.*, vol. V, no. 3, Aug. 1952, pp. 301-348.
10. Middleton, Wilbur D.; and Carlson, Harry W.: A Numerical Method for Calculating Near-Field Sonic-Boom Pressure Signatures. NASA TN D-3082, 1965.
11. Jones, L. B.: Lower Bounds for the Pressure Jump of the Bow Shock of a Supersonic Transport. *Aeronaut. Quart.*, vol. XXI, pt. 1, Feb. 1970, pp. 1-17.
12. Hayes, Wallace D.; Haefeli, Rudolph C.; and Kulsrud, H. E.: Sonic Boom Propagation in a Stratified Atmosphere, With Computer Program. NASA CR-1299, 1969.
13. Warren, C. H. E.: A Significant Single Quantity That Typifies a Sonic Bang. *J. Acoust. Soc. America*, vol. 51, no. 1, pt. 2, Jan. 1972, pp. 418-420.

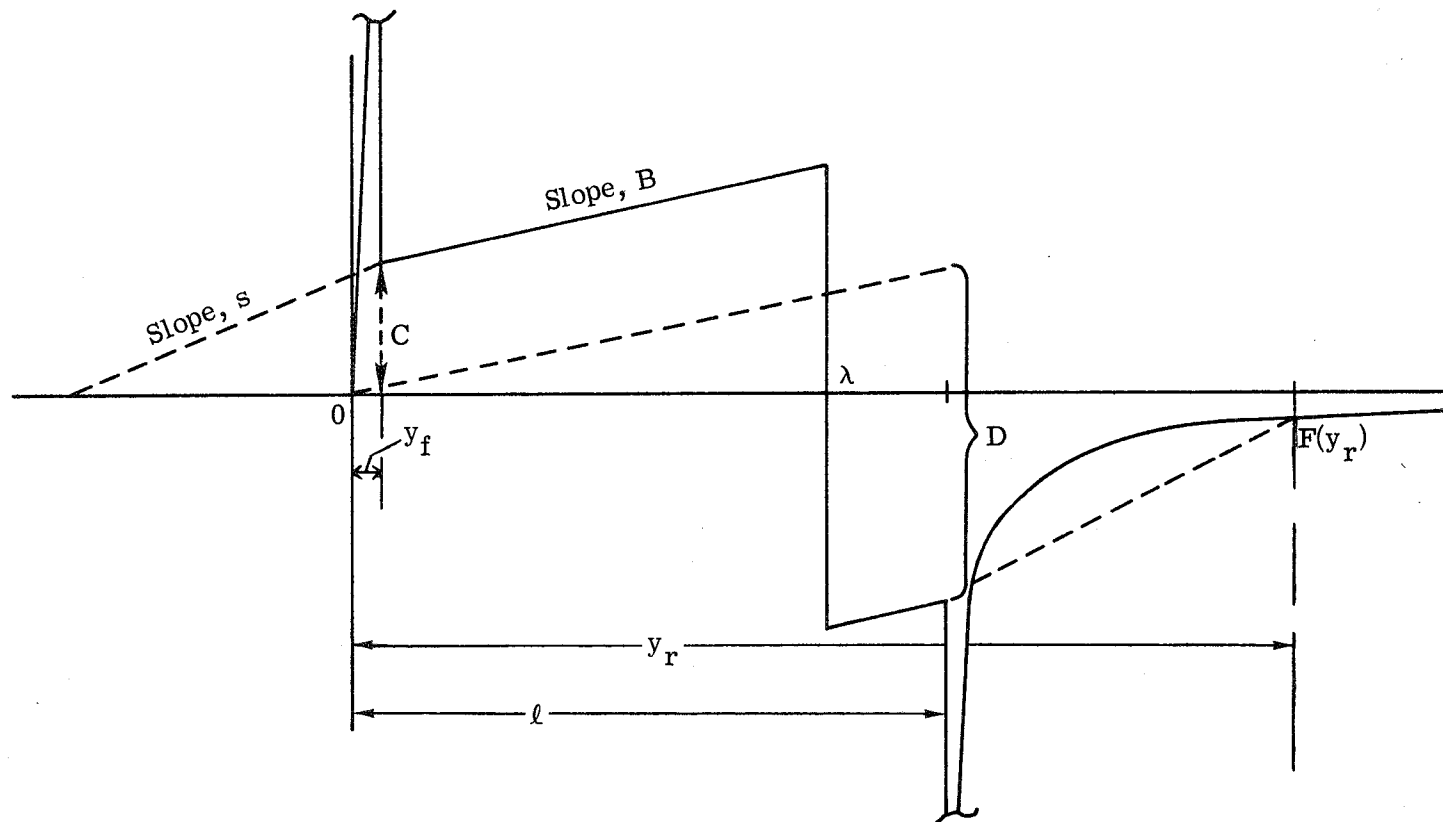


Figure 1.- Assumed form of the F-function in the minimization scheme.

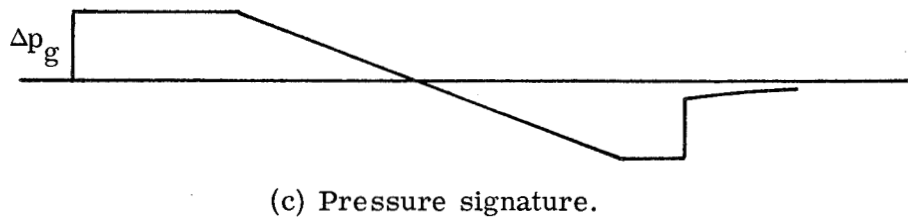
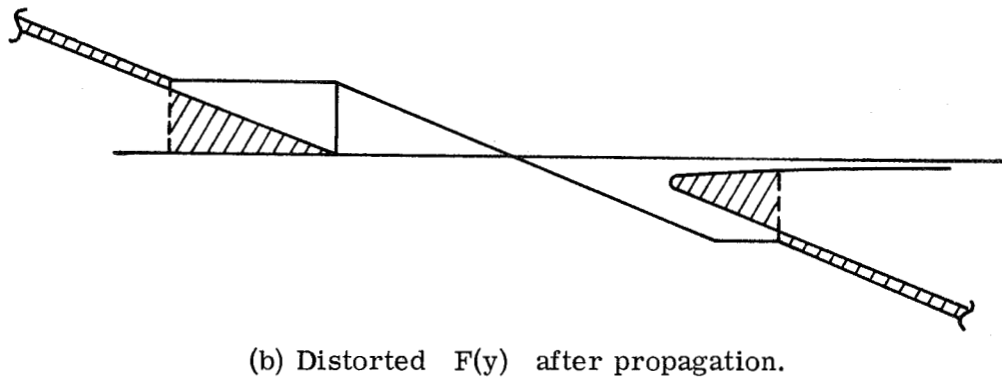
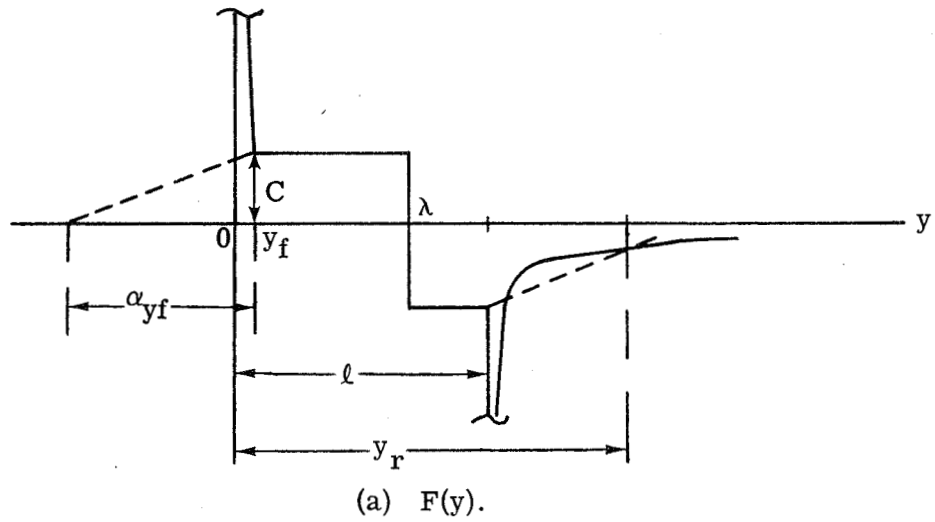
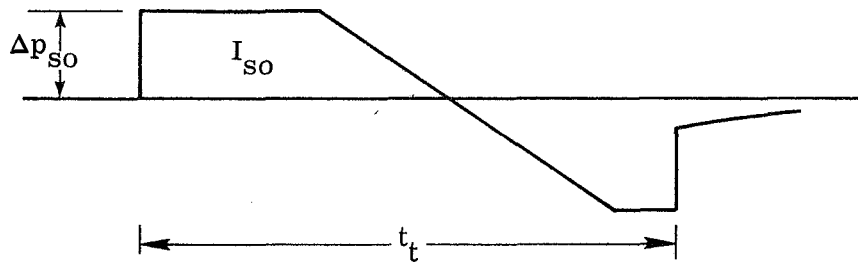
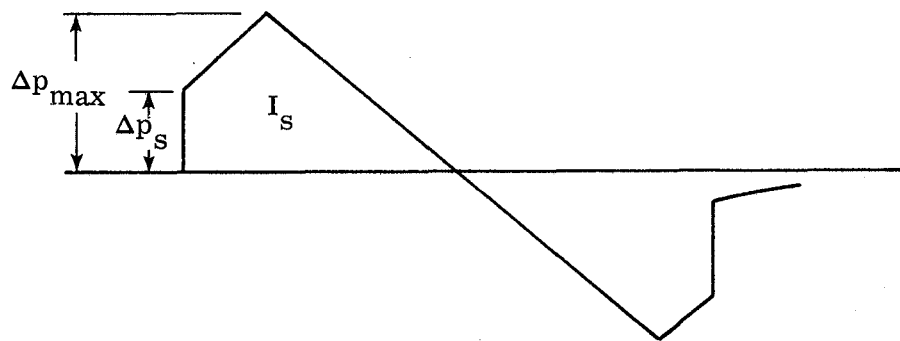


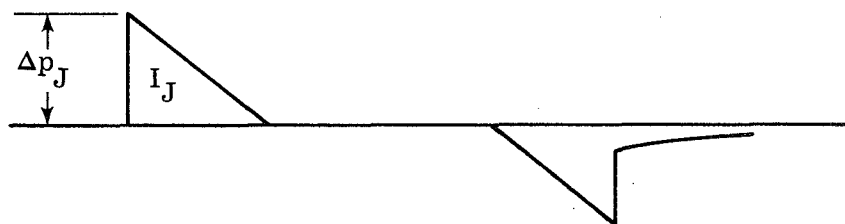
Figure 2.- Area-balancing method of changing $F(y)$ to a pressure signature.



(a) Minimum overpressure signature. $B = 0$.

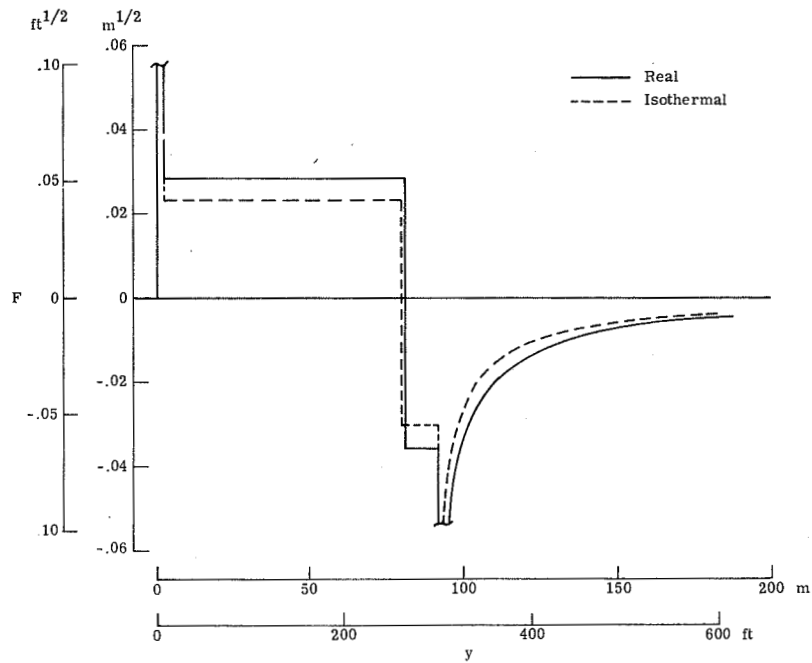


(b) Minimum shock signature. $0 < B < s$.

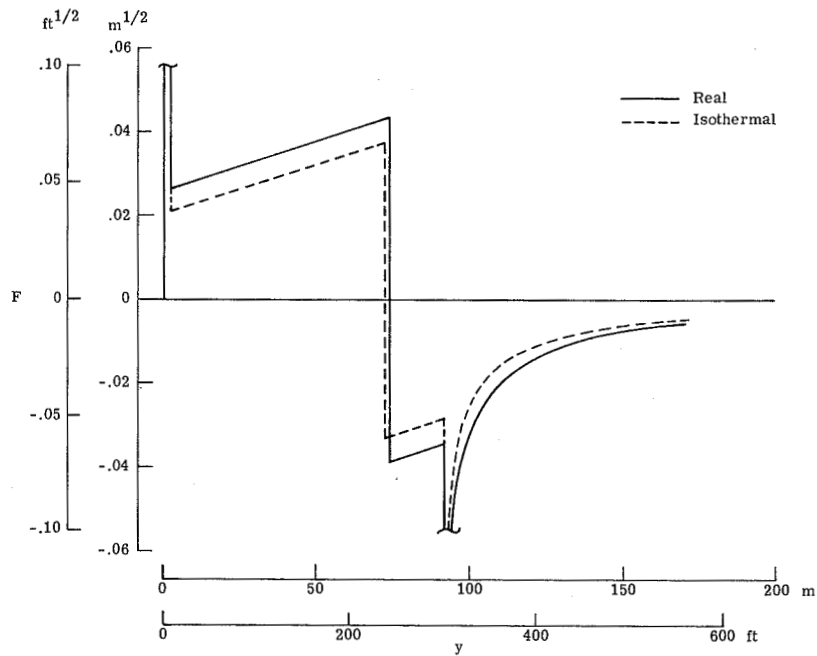


(c) Minimum impulse signature.

Figure 3.- Types of signatures considered. $\Delta p_c = 4I/t_t$.

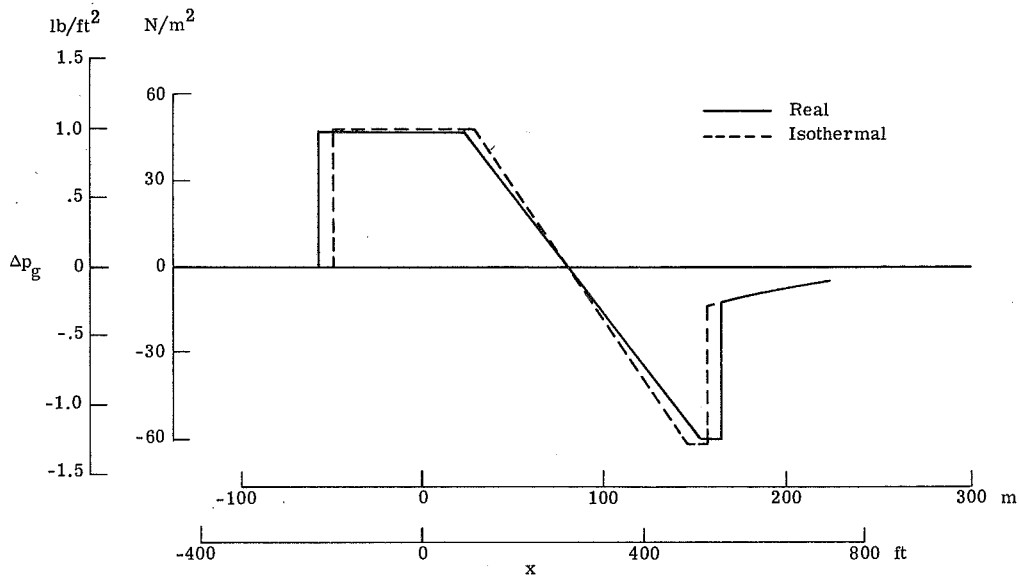


(a) F-function corresponding to minimum overpressure signature.

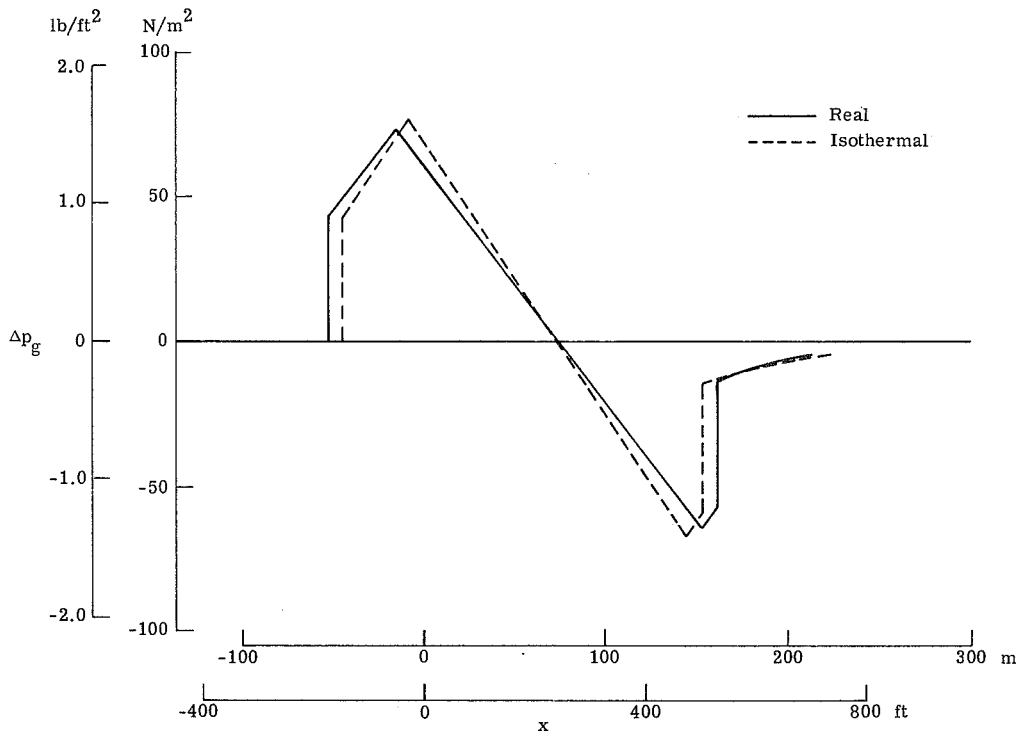


(b) F-function corresponding to minimum shock signature.

Figure 4.- Minimizing F-functions. $M = 2.7$; $h = 18\,288$ m (60 000 ft); $W = 272\,155$ kg (600 000 lb); $\ell = 91.44$ m (300 ft); $P_f/P_r = 1$; $K = 2$; $H = 7620$ m (25 000 ft).

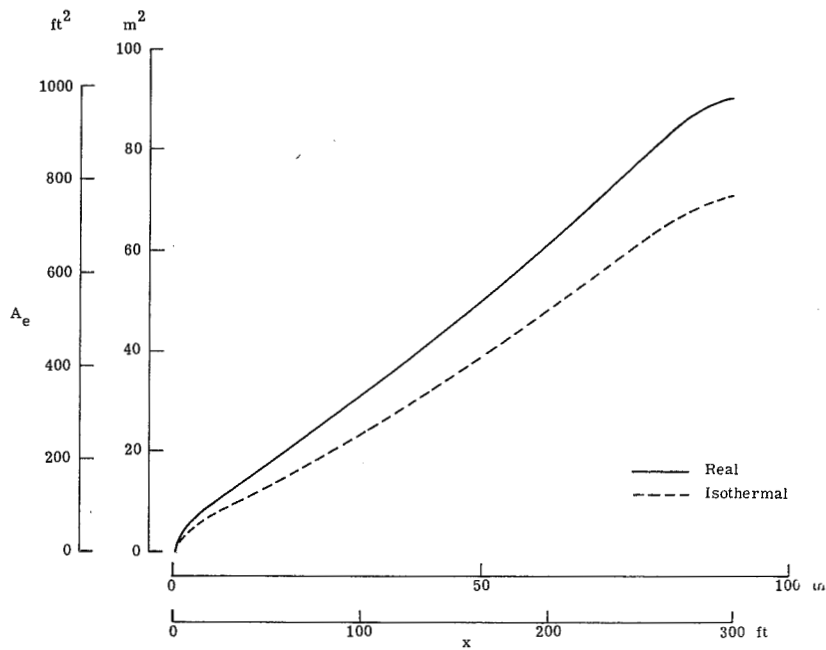


(a) Minimum overpressure signature.

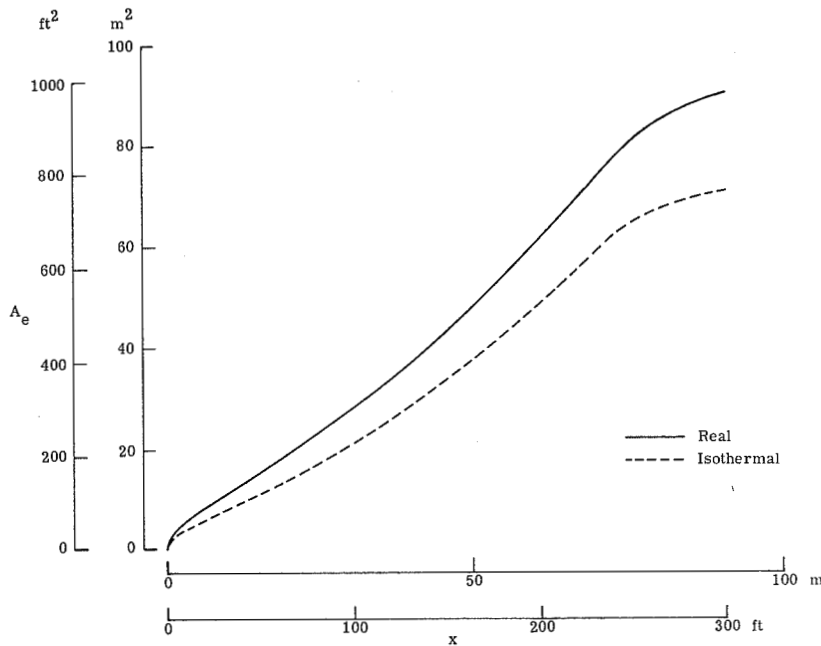


(b) Minimum shock signature.

Figure 5.- Minimizing pressure signatures. $M = 2.7$; $h = 18\,288\text{ m}$ (60 000 ft); $W = 272\,155\text{ kg}$ (600 000 lb); $\ell = 91.44\text{ m}$ (300 ft); $P_f/P_r = 1$; $K = 2$; $H = 7620\text{ m}$ (25 000 ft).

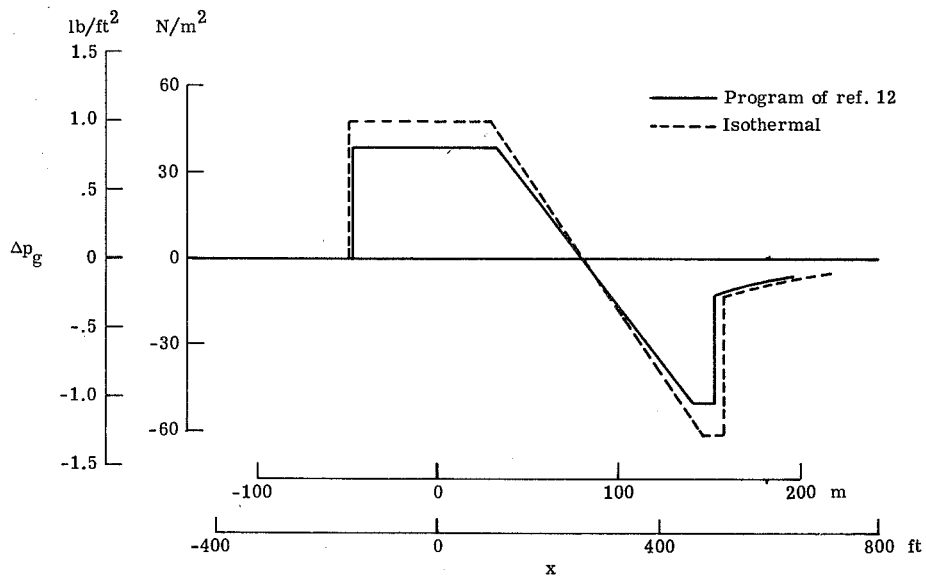


(a) Area distribution corresponding to minimum overpressure signature.

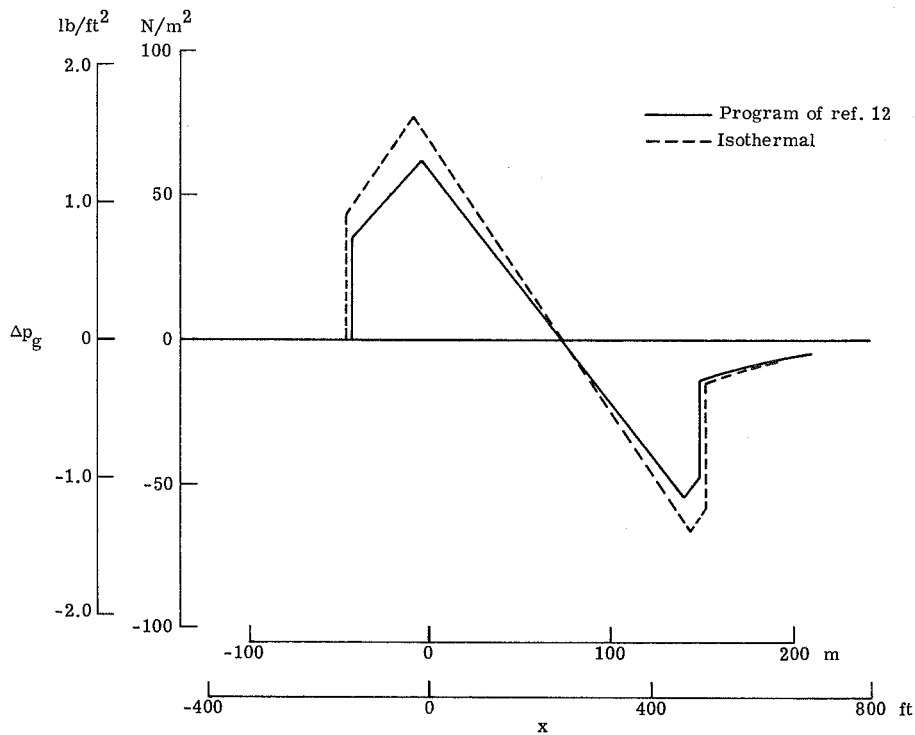


(b) Area distribution corresponding to minimum shock signature.

Figure 6.- Minimizing equivalent area distributions. $M = 2.7$; $h = 18\,288\text{ m}$ (60 000 ft); $W = 272\,155\text{ kg}$ (600 000 lb); $\ell = 91.44\text{ m}$ (300 ft); $P_f/P_r = 1$; $K = 2$; $H = 7620\text{ m}$ (25 000 ft).

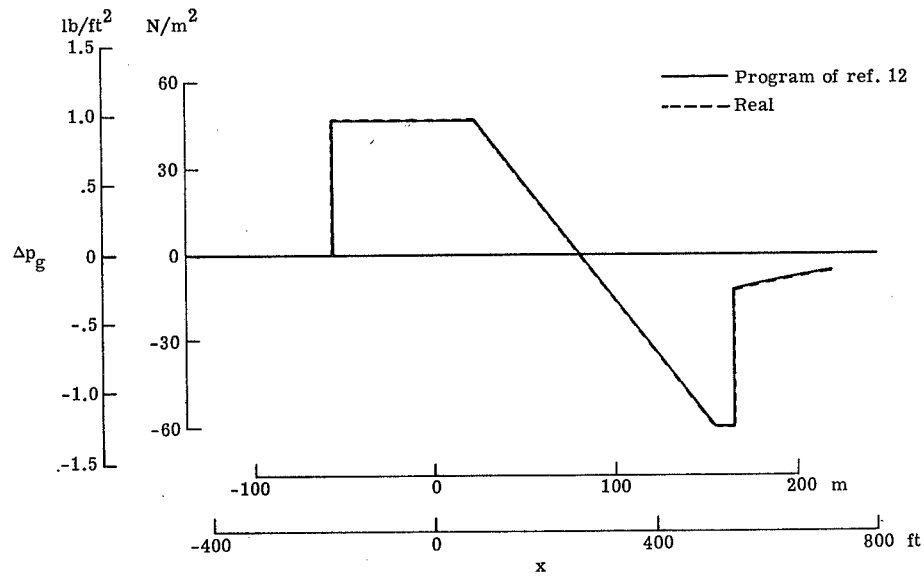


(a) Minimum overpressure signature.

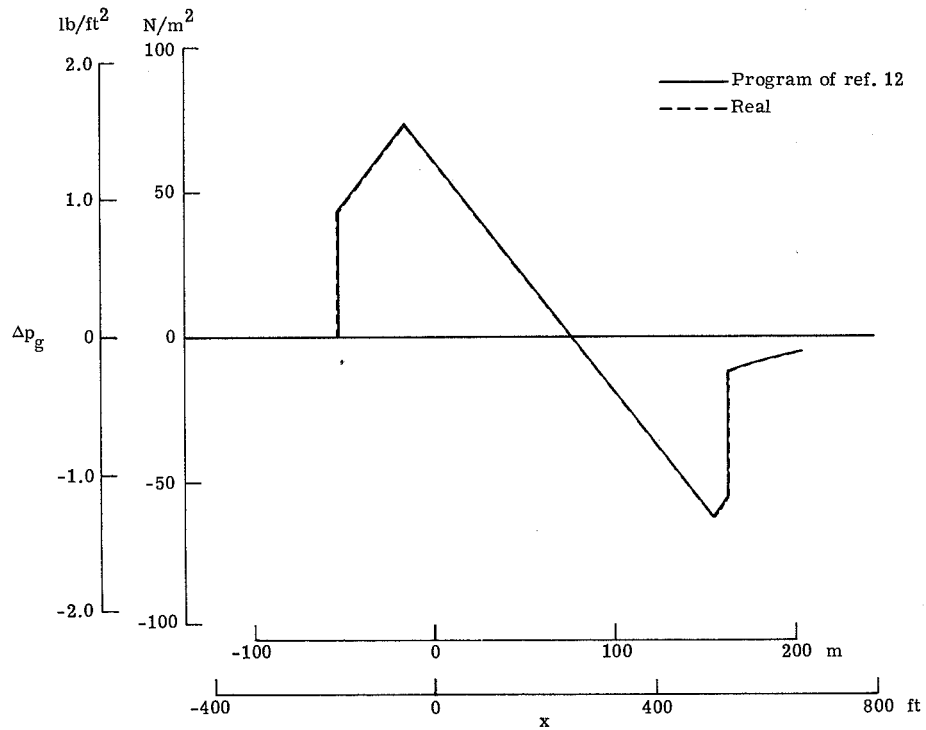


(b) Minimum shock signature.

Figure 7.- Predictions obtained with isothermal atmosphere minimization program and with program of reference 12. $M = 2.7$; $h = 18\,288\text{ m}$ (60 000 ft); $W = 272\,155\text{ kg}$ (600 000 lb); $l = 91.44\text{ m}$ (300 ft); $P_f/P_r = 1$; $K = 2$; $H = 7620\text{ m}$ (25 000 ft).



(a) Minimum overpressure signature.



(b) Minimum shock signature.

Figure 8.- Predictions obtained with real atmosphere minimization program and with program of reference 12. $M = 2.7$; $H = 18\,288\text{ m}$ (60 000 ft); $W = 272\,155\text{ kg}$ (600 000 lb); $\ell = 91.44\text{ m}$ (300 ft); $P_f/P_r = 1$; $K = 2$; $H = 7620\text{ m}$ (25 000 ft).

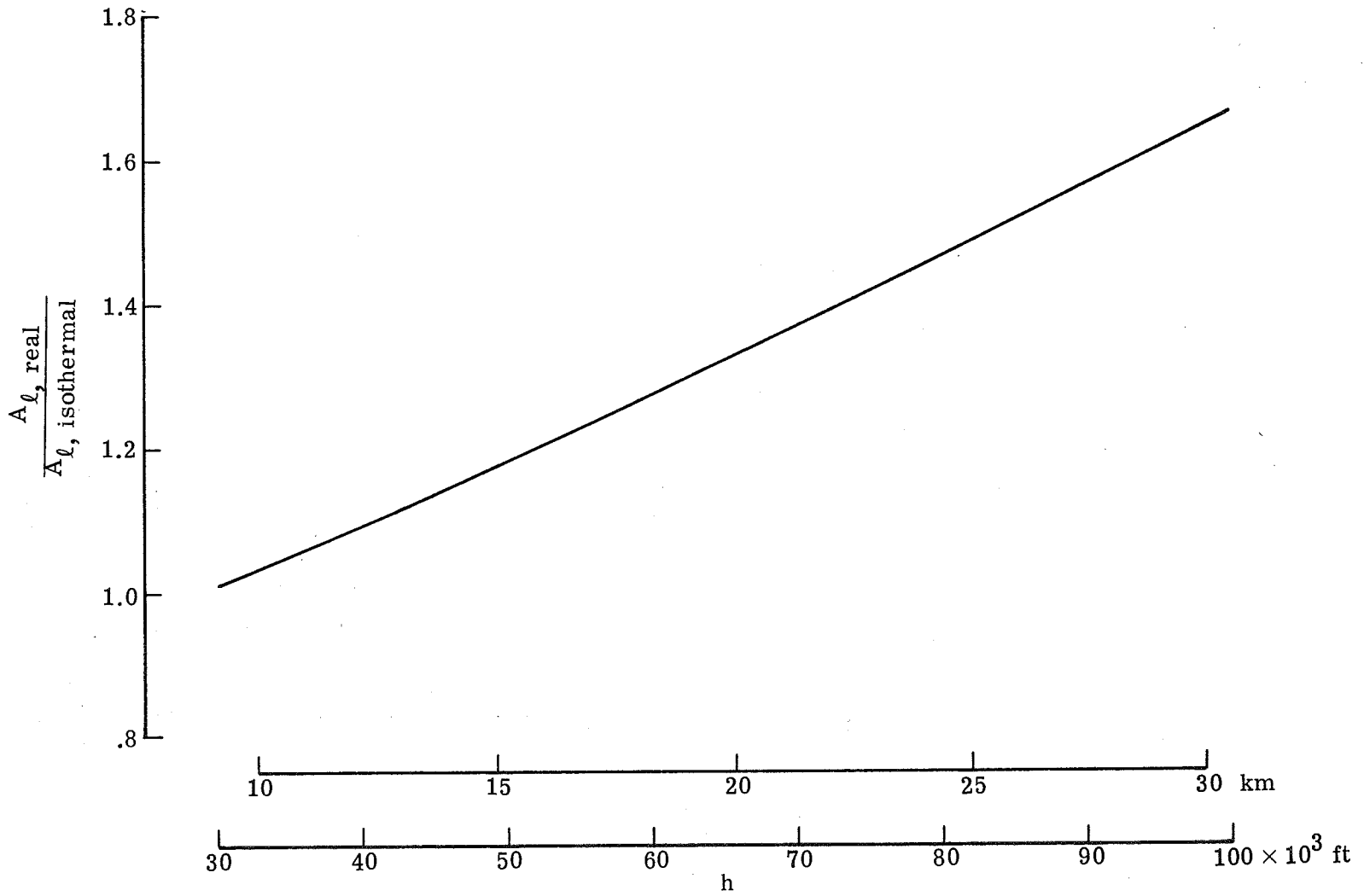
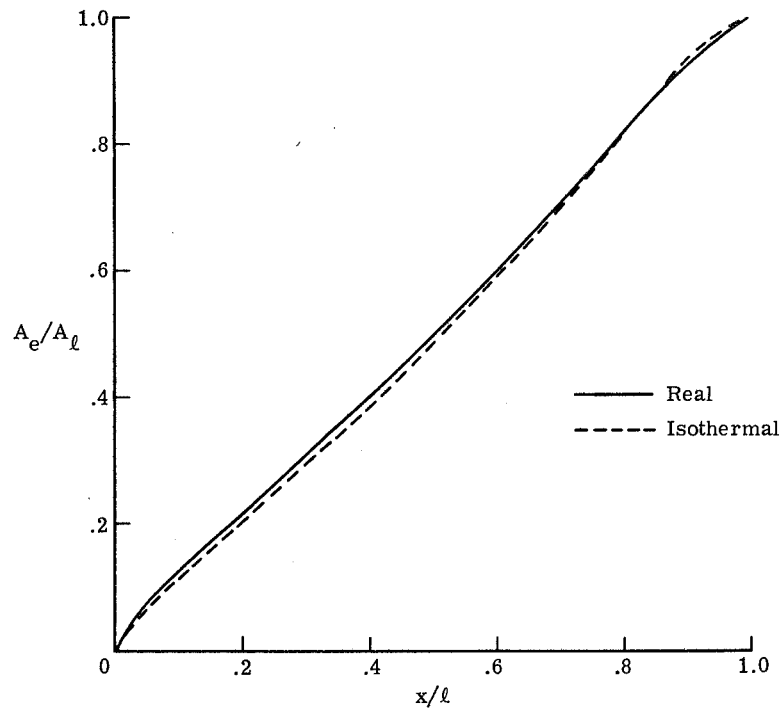
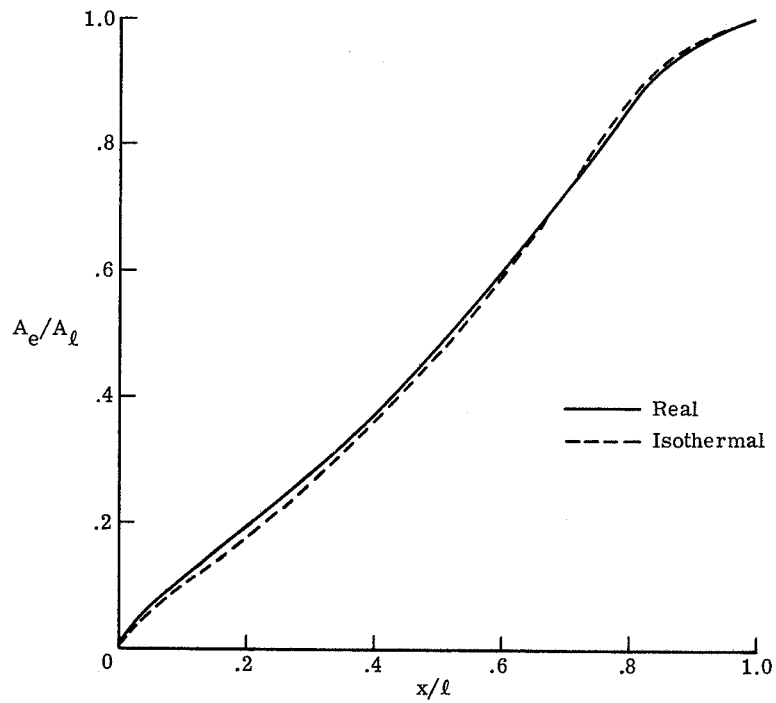


Figure 9.- Correction factor for isothermal area distribution when $H = 7620 \text{ m}$ ($25\,000 \text{ ft}$).

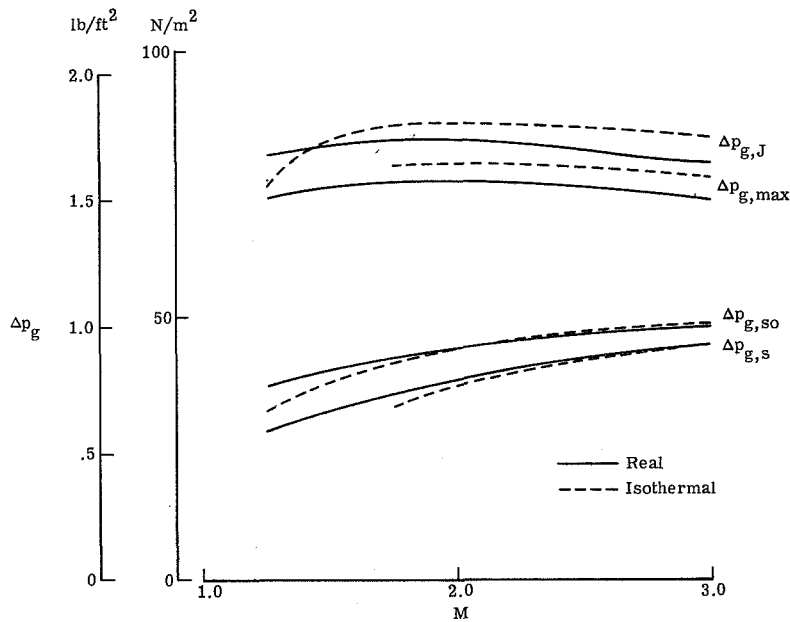


(a) Area distribution corresponding to minimum overpressure signature.

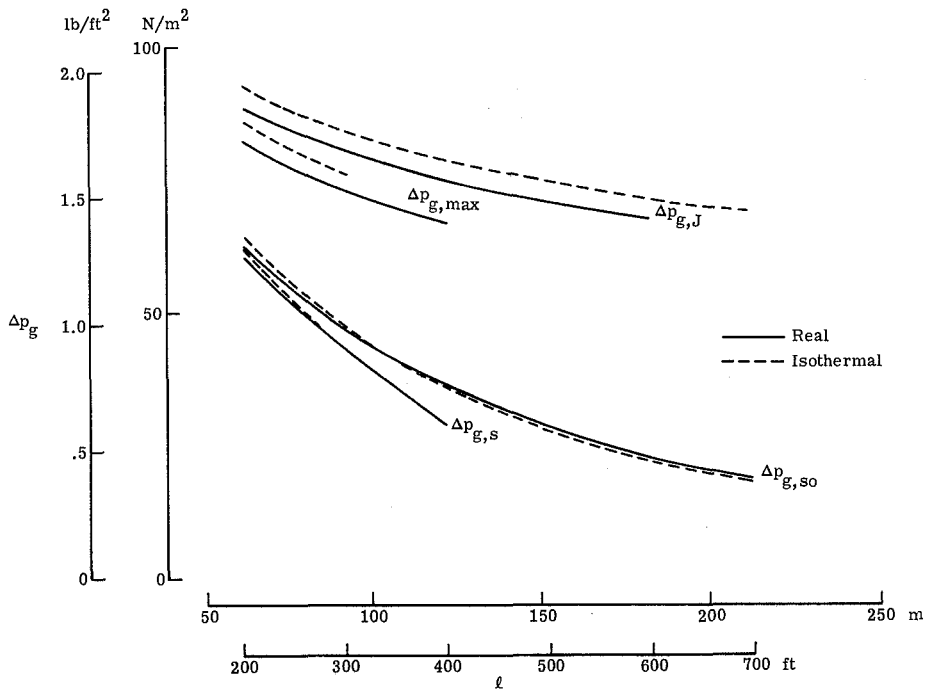


(b) Area distribution corresponding to minimum shock signature.

Figure 10.- Normalized area distributions.



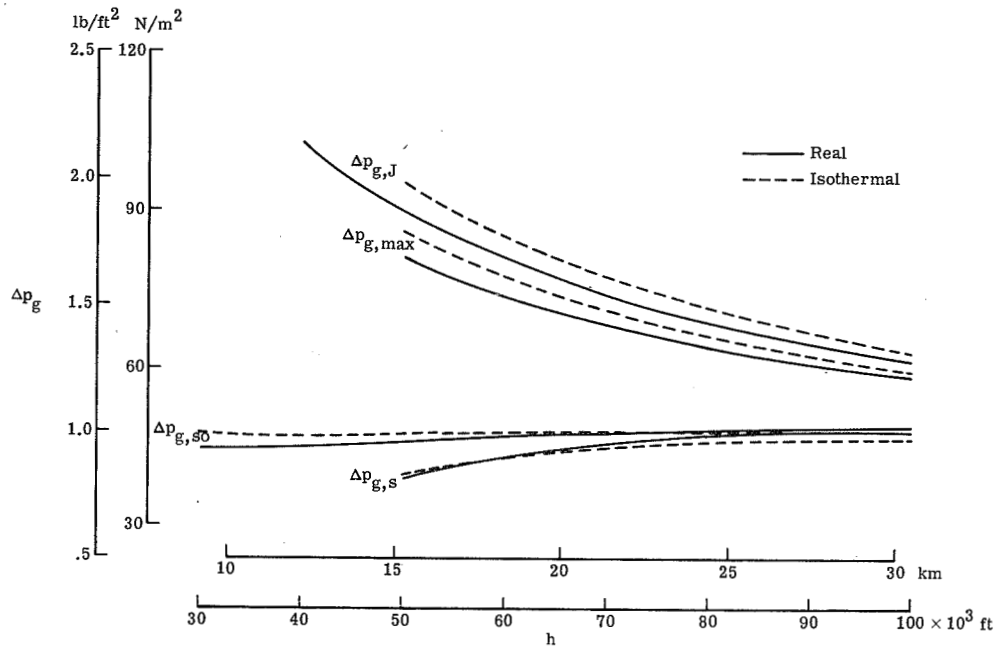
(a) Overpressure as a function of Mach number. $h = 18\,288\text{ m}$ (60 000 ft);
 $W = 272\,155\text{ kg}$ (600 000 lb); $\ell = 91.44\text{ m}$ (300 ft).



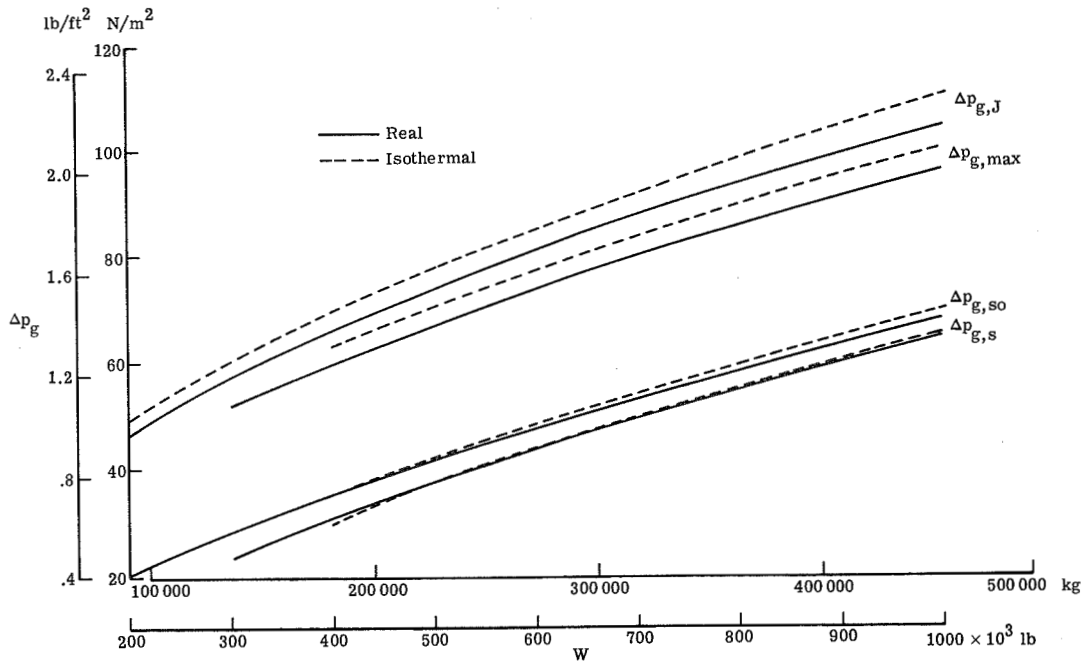
(b) Overpressure as a function of equivalent airplane length. $M = 2.7$;
 $h = 18\,288\text{ m}$ (60 000 ft); $W = 272\,155\text{ kg}$ (600 000 lb).

Figure 11.- Comparison of ground overpressures for real and isothermal atmospheres.

$$P_f/P_r = 1; \quad K = 2; \quad H = 7620\text{ m} (25\,000\text{ ft}).$$

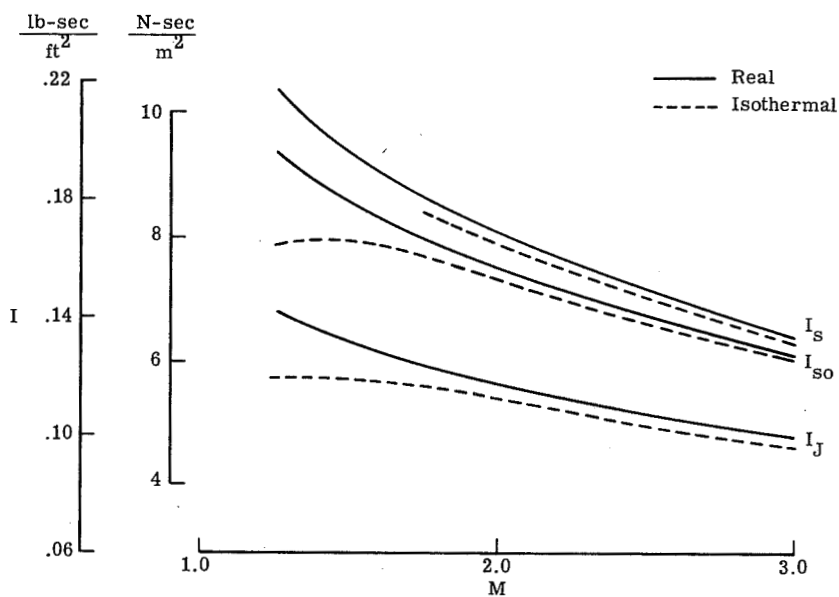


(c) Overpressure as a function of altitude. $M = 2.7$; $W = 272\ 155$ kg (600 000 lb);
 $\ell = 91.44$ m (300 ft).

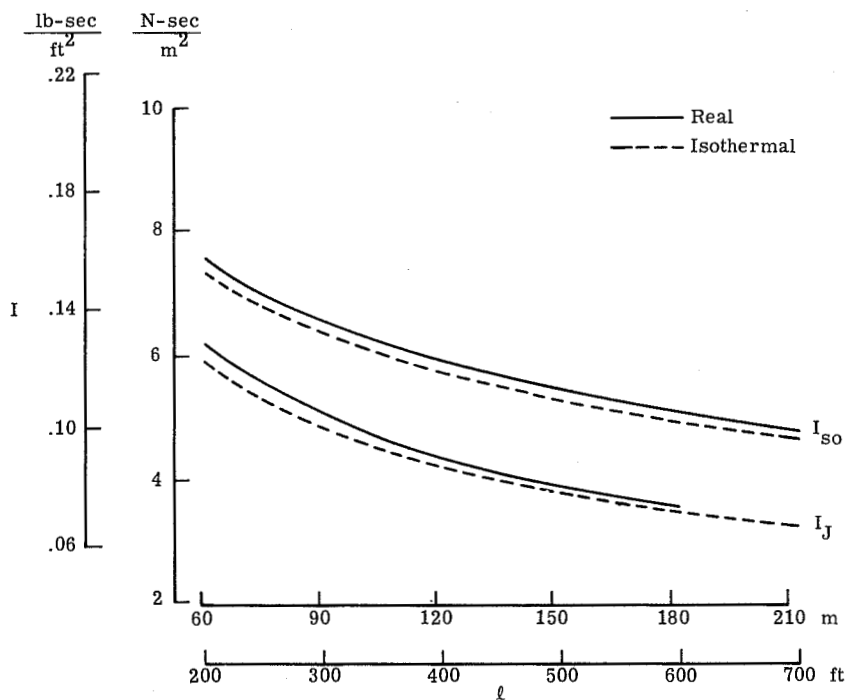


(d) Overpressure as a function of airplane weight. $M = 2.7$; $h = 18\ 288$ m (60 000 ft);
 $\ell = 91.44$ m (300 ft).

Figure 11.- Concluded.



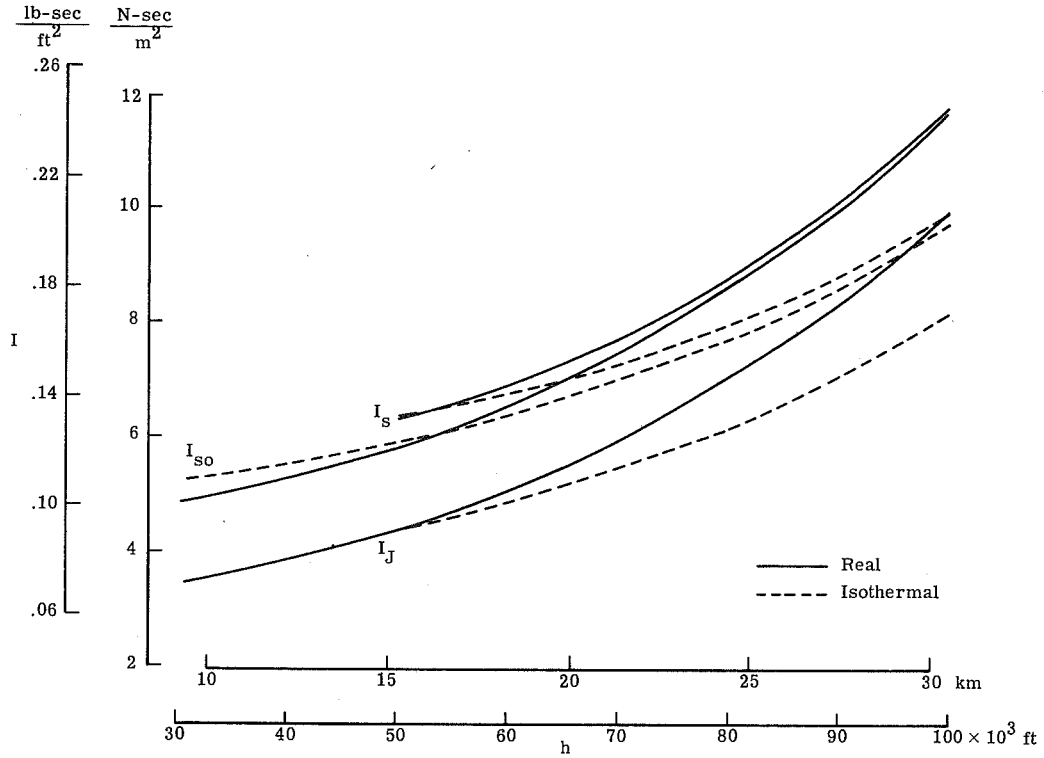
(a) Impulse as a function of Mach number. $h = 18\,288\text{ m}$ (60 000 ft);
 $W = 272\,155\text{ kg}$ (600 000 lb); $\ell = 91.44\text{ m}$ (300 ft).



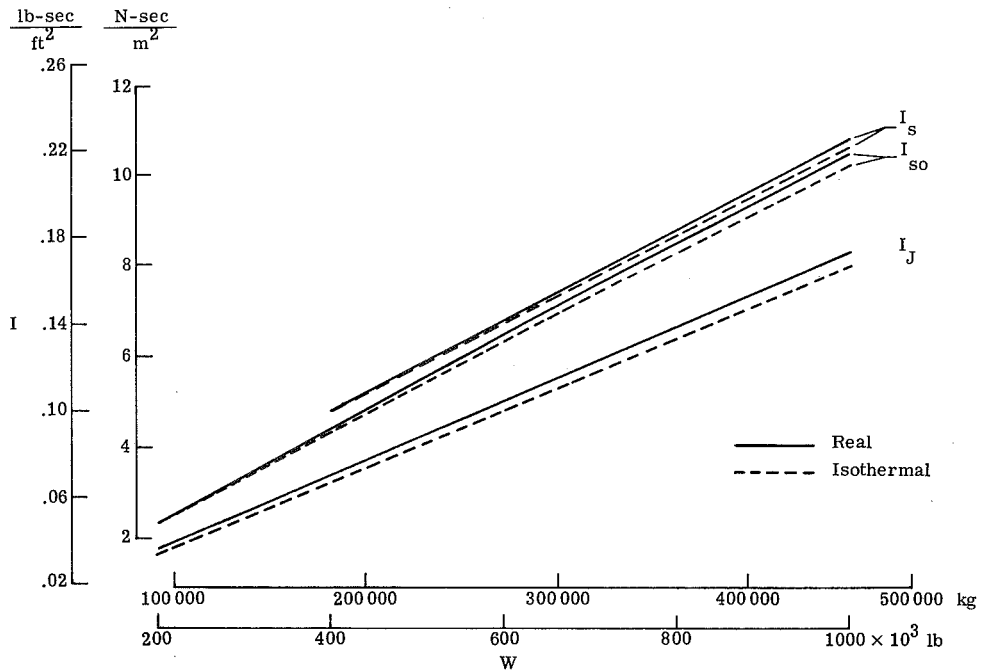
(b) Impulse as a function of equivalent length of airplane. $M = 2.7$;
 $h = 18\,288\text{ m}$ (60 000 ft); $W = 272\,155\text{ kg}$ (600 000 lb).

Figure 12.- Comparison of impulses for real and isothermal atmospheres.

$$P_f/P_r = 1; K = 2; H = 7620\text{ m} (25\,000\text{ ft}).$$

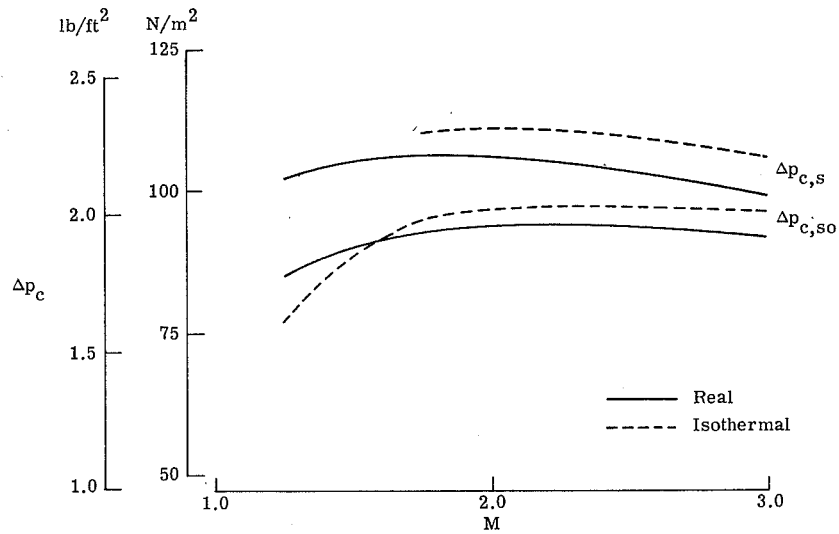


(c) Impulse as a function of altitude. $M = 2.7$; $W = 272\ 155$ kg (600 000 lb);
 $\ell = 91.44$ m (300 ft).

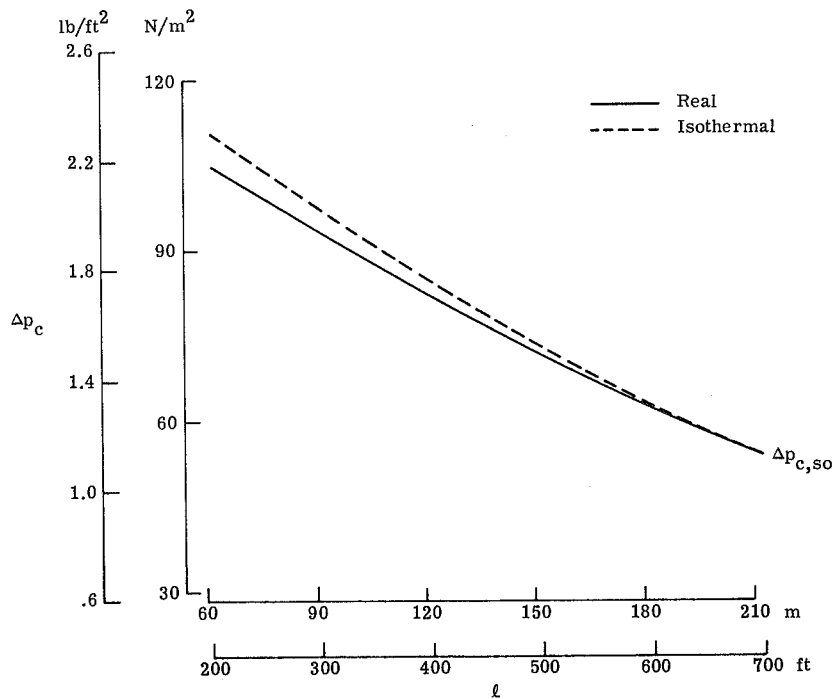


(d) Impulse as a function of weight. $M = 2.7$; $h = 18\ 288$ m (60 000 ft);
 $\ell = 91.44$ m (300 ft).

Figure 12.- Concluded.

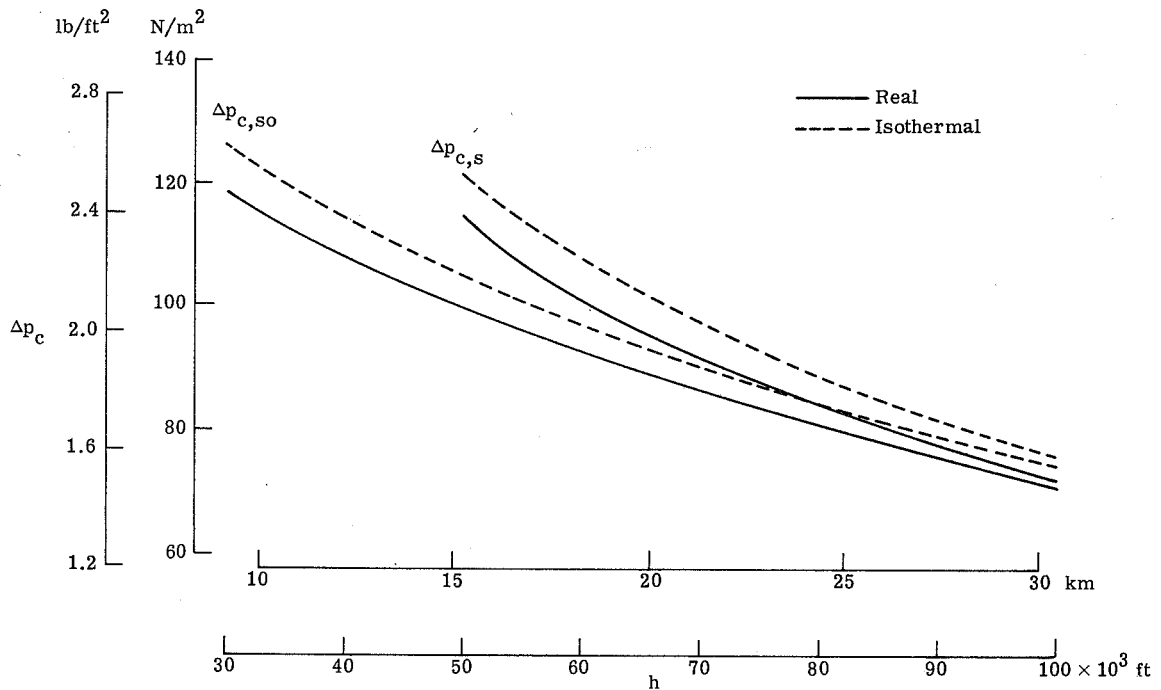


(a) Characteristic overpressure as a function of Mach number.
 $h = 18\,288\text{ m}$ (60 000 ft); $W = 272\,155\text{ kg}$ (600 000 lb);
 $\ell = 91.44\text{ m}$ (300 ft).

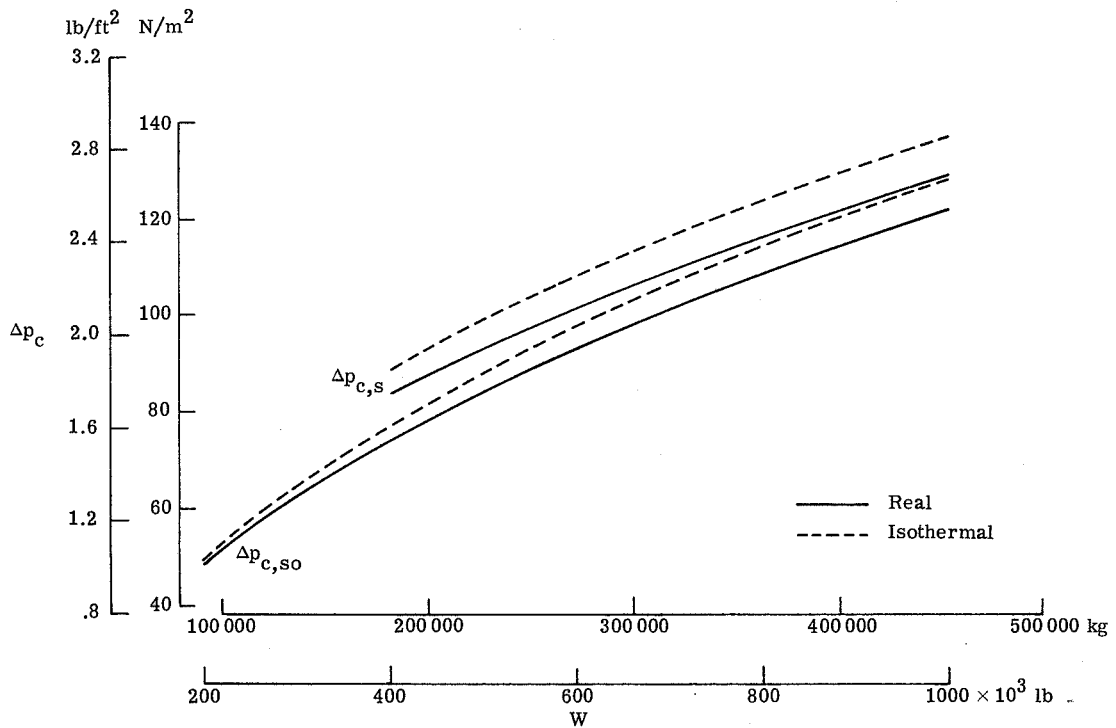


(b) Characteristic overpressure as a function of length. $M = 2.7$;
 $h = 18\,288\text{ m}$ (60 000 ft); $W = 272\,155\text{ kg}$ (600 000 lb).

Figure 13.- Comparison of characteristic overpressures for real and isothermal atmospheres. $P_f/P_r = 1$; $K = 2$; $H = 7620\text{ m}$ (25 000 ft).



(c) Characteristic overpressure as a function of altitude. $M = 2.7$;
 $W = 272\,155\text{ kg}$ (600 000 lb); $\ell = 91.44\text{ m}$ (300 ft).



(d) Characteristic overpressure as a function of weight. $M = 2.7$;
 $h = 18\,288\text{ m}$ (60 000 ft); $\ell = 91.44\text{ m}$ (300 ft).

Figure 13.- Concluded.

20
NATIONAL AERONAUTICS AND SPACE ADMINISTRATION
WASHINGTON, D.C. 20546

OFFICIAL BUSINESS
PENALTY FOR PRIVATE USE \$300

**SPECIAL FOURTH-CLASS RATE
BOOK**

POSTAGE AND FEES PAID
NATIONAL AERONAUTICS AND
SPACE ADMINISTRATION
451



HQ SAMTEC, AFL 2827
TECHNICAL LIBRARY (PMET)
VANDENBERG AFB, CA 93437.



POSTMASTER: If Undeliverable (Section 158
Postal Manual) Do Not Return

"The aeronautical and space activities of the United States shall be conducted so as to contribute . . . to the expansion of human knowledge of phenomena in the atmosphere and space. The Administration shall provide for the widest practicable and appropriate dissemination of information concerning its activities and the results thereof."

—NATIONAL AERONAUTICS AND SPACE ACT OF 1958

NASA SCIENTIFIC AND TECHNICAL PUBLICATIONS

TECHNICAL REPORTS: Scientific and technical information considered important, complete, and a lasting contribution to existing knowledge.

TECHNICAL NOTES: Information less broad in scope but nevertheless of importance as a contribution to existing knowledge.

TECHNICAL MEMORANDUMS: Information receiving limited distribution because of preliminary data, security classification, or other reasons. Also includes conference proceedings with either limited or unlimited distribution.

CONTRACTOR REPORTS: Scientific and technical information generated under a NASA contract or grant and considered an important contribution to existing knowledge.

TECHNICAL TRANSLATIONS: Information published in a foreign language considered to merit NASA distribution in English.

SPECIAL PUBLICATIONS: Information derived from or of value to NASA activities. Publications include final reports of major projects, monographs, data compilations, handbooks, sourcebooks, and special bibliographies.

TECHNOLOGY UTILIZATION PUBLICATIONS: Information on technology used by NASA that may be of particular interest in commercial and other non-aerospace applications. Publications include Tech Briefs, Technology Utilization Reports and Technology Surveys.

Details on the availability of these publications may be obtained from:

SCIENTIFIC AND TECHNICAL INFORMATION OFFICE

NATIONAL AERONAUTICS AND SPACE ADMINISTRATION
Washington, D.C. 20546